A Computational Science Approach to Understanding Human Conflict

D. Dylan Johnson Restrepo, Physics Department, George Washington University, Washington D.C. 20052, U.S.A.

Michael Spagat, Economics Department, Royal Holloway University of London, Egham, Surrey TW20 0EX, U.K.

Stijn van Weezel, Economics Department, Radboud University, Nijmegen, Netherlands

Minzhang Zheng, Biomedical Engineering, Michigan State University, East Lansing, MI 48824, U.S.A.

Neil F. Johnson, Physics Department, George Washington University, Washington D.C. 20052, U.S.A.

Abstract

We discuss how computational data science and agent-based modeling, are shedding new light on the age-old issue of human conflict. While social science approaches focus on individual cases, the recent proliferation of empirical data and complex systems thinking has opened up a computational approach based on identifying common statistical patterns and building generative but minimal agent-based models. We discuss a reconciliation for various disparate claims and results in the literature that stand in the way of a unified description and understanding of human wars and conflicts. We also discuss the unified interpretation of the origin of these power-law deviations in terms of dynamical processes. These findings show that a unified computational science framework can be used to understand and quantitatively describe collective human conflict.

The proliferation of large empirical datasets has opened up a new computational science approach toward understanding one of the core puzzles of sociology: collective human conflict towards other humans in the form of warfare and terrorism. This computational focus is still viewed with some suspicion in the social sciences because of its unfamiliar aim of seeking a system-level understanding across conflicts, as opposed to a drill-down narrative for a specific conflict. However, one of the more remarkable results that has emerged from this computational approach, is the finding that the distribution of the aggregate numbers of fatalities in entire wars and conflicts (i.e. the distribution of their sizes) can be well modeled as an approximate power-law (Cederman, 2003; González-Val, 2016; Clauset, 2018). This empirical regularity is known as Richardson's Law — after polymath Lewis Fry Richardson who first studied this phenomenon more than half a century ago (Richardson, 1948, 1960). Separate work has shown that approximate power laws also tend to capture well the distributions of event sizes, measured by fatality counts, *within* wars (Bohorquez et al., 2009; Johnson et al., 2013; Spagat et al., 2018) and terrorism (Spagat et al., 2018; Clauset et al., 2007). Moreover an explanatory generative, multi-agent model has been suggested (Bohorquez et al., 2009).

Here we draw together various distinct results to date in this area, including published and unpublished works of ours. We discuss a novel, unifying analysis of the computational science results to date, and the agent-based model that helps explain them. The scientific approach that we adopt in this particularly difficult area of human conflict, is a computational science one in that we start with no theoretical hypothesis and instead simply observe the data, taking in as much as we can into our analysis as opposed to simply sampling from it. We describe the hidden statistical patterns following Bohorquez et al. (2009), Johnson et al. (2013) and Spagat et al. (2018) based on computational analyses of the datasets. We then discuss three contributions that open up a unified understanding of human conflict. First, we discuss how the approximate power laws obtained *across* wars, treating the number of fatalities in each war as a single data point, bear a simple relationship to the approximate power laws found *within* single wars. More precisely, we use simulations to show that the ranges of power-law exponents found within individual conflicts will, when we aggregate the event data they generate into complete wars, produce the sorts of power-law exponents researchers have found across whole wars (Figs. 1-3). This insight overturns apparent assumptions in the literature

(see for example Clauset (2018)) that the behavior over aggregated conflicts is somehow separate from the behavior within wars, due to their different power-law exponents. Second, we highlight a common feature of conflict event data that is often ignored, leading some researchers to exaggerate evidence against power laws in some conflicts. Third, we explain that the generative theory of human conflict in Bohorquez et al. (2009) does not assume pure power-law behavior. On the contrary, it is far more general: specifically, it describes and explains approximate power-laws when they exist, but also it is able to explain observed departures from power laws in terms of microscopic dynamical processes. The Appendix provides a stripped-down, simplified version of this mathematical model that explicitly reproduces the common statistical power-law feature (i.e. an exponent near 2.5) that seems to arise for all human conflict – from wars to terrorism as shown in Figs. 1-3.

1 Computational Science Approach

Our focus is on collective phenomena since complex systems thinking suggests that if there are interesting patterns, then they are more likely to emerge in activities that involve a larger collection of people. Just as traffic jam patterns are known to occur similarly in cities across the world, despite the differences in the people involved, the mechanical details of their cars, and the environmental factors, it seems that the sheer fact of having to self-organize in a way that avoids being found out or apprehended, might lie behind some hidden systematic patterns. In short, the crowd behavior of how humans collectively 'do' terrorism and insurgency – and hence in general commit violent acts – might be expected show some form of universality. In our analysis the size s of a discrete event, such as a suicide bombing or an attack, is defined as the number of people killed in the event, which is termed the severity of the event.

Figures 1-2 arise from analyzing the latest version of the empirical event data on armed conflict and terrorism in the Georeferenced Event Dataset (GED) of the Uppsala Conflict Data Programme. This is the most comprehensive and accurate georeferenced dataset available. We then perform the same analysis of terrorist incidents (Fig. 3) using the Global Terrorism Database (GTD, the 2017 version), provided by the National Consortium for the Study of

Terrorism and Responses to Terrorism (START). This GTD dataset includes both trans/inter-national and domestic terrorist incidents, and is updated annually. It provides the most comprehensive publicly available dataset on terrorist events. It covers the period from 1970 to 2016 and includes detailed information on incident times, locations, fatality counts and, when identifiable, the perpetrating group or individual. We include only events that are, according to the coding, definitely acts of terrorism causing at least one fatality and that are attributed to a known organization that has perpetrated at least 30 attacks. Also, we only use events occurring after 1997 because the GTD coding procedures changed in that year. This provides us with $16,399$ terrorist attacks between $1998-2016$, carried out by 60 groups.

Our computational approach uses Gillespie's *poweRlaw* software package in R (see Gillespie (2015)) to fit the model $Ms^{-\alpha}$ to the distributions of the event severities above an estimated cut-off value s_{min} using maximum likelihood estimation. M is a constant, s is the size of the event (i.e. severity in our analysis, which is the number killed in the event), and α is called the power-law exponent. Following the standard procedure, the minimum cut-off s_{min} is estimated using a Kolmogorov-Smirnov approach which minimizes the distance between the cumulative density function of the data and the fitted model. The estimates are obtained using a bootstrap procedure with 1,000 iterations, in order to account for parameter uncertainty.

Figure 1 illustrates the power-law distribution emerging for the histogram of the severity of conflict events. Such a power-law distribution emerges frequently in the study of collective behavior in systems of interacting objects (which could include humans) when there are complex feedback mechanisms at play. For human events such as in conflicts and terrorism, there will also likely be such feedback processes during the attack preparation and execution. The opposite case to this is a process that has no feedback, like the outcome from tossing a coin, producing a Normal distribution. Figures 2 and 3 show the exponent values α for the power-laws across conflicts and across terrorist organizations' campaigns respectively. They all tend to be clustered near the exponent value $\alpha = 2.5$.

Having looked at computational patterns for events within a given conflict or terrorist campaign, we now turn to consider patterns across conflicts, i.e. where each conflict now provides one datapoint obtained by summing up the casualties from all the events within the conflict. It has been shown by

Cederman (2003), Clauset (2018) and most recently Braumoeller (2019), that the distribution of severities for entire wars is an approximate power-law within an estimated range of $\alpha \sim 1.5 - 1.7$, depending on the date range and war types included. The goodness-of-fit values seem to be fairly high as well ($p \sim 0.5$). However as shown above, events within each *individual* war i show an approximate power-law distribution which is spread broadly around an exponent value of $\beta_i \sim 2.5$, again with reasonably high p values. The question therefore arises: are these two findings for the power-law test for (i) aggregate wars yielding exponent $\alpha \sim 1.5 - 1.7$ and (ii) individual wars yielding exponents $\{\beta_i\} \sim 2.5$, consistent with each other? Below we show through computer simulations that they are indeed consistent. Thus, we provide the first unified treatment of human conflict that crosses the boundary separating fatality events within individual wars from aggregated fatality totals across entire wars.

To show this, we first simulate a set of individual events for an individual war i (see Fig. 4). Though we could in principle generate these events using the cluster interactions from our generative model discussed later on, or its more basic one-dimensional version in the Appendix, for simplicity for a given war i we instead choose to generate random events from a power-law with exponent β_i, where β_i is picked randomly from a distribution spread around 2.5. We then repeat this procedure to generate a number of different simulated wars, allowing a different number of events n for each war. We have checked the robustness of our results for different choices of peaked distribution for these β_i values, and also different choices of $s_{\min}$ for the power-law onset. Here for simplicity, we show results for a normal distribution of β_i values. We have also checked that our results are robust to different choices of standard deviation in β_i around 2.5. We have also checked the robustness for having a peak away from 2.5, and we have checked the robustness to having different numbers of events for each simulated model war i.

In all cases, we find that the results that we provide in Fig. 4 are indeed representative and the core finding is robust. The aggregated casualty total for each war i is given by W_i which is the sum of the individual events $1, 2, ..$ etc. within that war, i.e. $W_i = s_1^i + s_2^i + ...$ This is shown schematically in Figs. 4(a) and (b). This entire process provides us with a set of values $\{W_i\}$ corresponding to the total fatalities in our simulated model wars $i = 1, 2, ...$ This represents our model's predicted record for all human wars. In the real world, only some prior wars have data available for them. Indeed, some

wars may have been lost from the history books and hence their existence is unknown. We therefore sample subsets of $\{W_i\}$ in order to mimic the known history books, and hence mimic the existing database of wars analysed by other researchers. We then proceed as if with real data, by doing the usual power-law test.

Fig. 4(c) shows the striking result that the resulting distribution of entire war exponents for different samples tends to be bunched in the same range $\alpha \sim 1.5 - 1.7$ as in the empirical findings. Moreover, the goodness-of-fit values are distributed around $p \sim 0.5$. We chose for simplicity $x_{\min} = 1$, and the $\{\beta_i\}$ to be distributed normally with a mean at 2.5 and a standard deviation of 0.5, similar to the empirical findings in our previous work. We also chose the number of events per war to follow a lognormal distribution which is again consistent with actual war data (see Spagat et al. (2018) for statistical details and links to the original data and code) and we show the resulting α distributions for three representative values of the mean in Fig. 4(c). We also chose 1000 total wars $\{W_i\}$, and sampled subsets of size 100. Again, we checked that the results in Fig. 4 are robust to variations in each of these choices.

Figure 4(c) serves to unify the power-law testing results for event sizes within individual wars with the corresponding results for fatalities aggregated over entire wars. It therefore captures how the scaling coefficient changes moving from the intra-conflict level to the inter-conflict level. As a result, we see that looking at individual violent events within a single war is not the same as looking at individual wars within a collection of many wars, despite the fact that both phenomena can be captured reasonably well by power laws. In particular, it shows that compiling aggregate data across wars has the effect of lowering the value of the best-fit exponent.

Now that several researchers are repeating this approach of power-law testing of human conflict data, we feel it is prudent to provide a note of caution regarding best computational science practice: estimates of goodness-of-fit for power-laws based on publicly available datasets viewed as pure 'event data' can be misleading and wrong. This is because many such datasets mix together true events with composite events. Such entries are not single discrete events in which X *people* were killed. In fact, it may be closer to a composite of X *events* in which 1 person is killed. Indeed, many databases contain entries that are composites of multiple events. To take an example,

the commonly used GED (Georeferenced Event Database) developed by the Uppsala Conflict Data Program (UCDP), has many such entries. These are flagged in the dataset with a special indicator variable, (`event_clarity`), so they are relatively easy to exclude. While only 10% of the observations in this dataset are composite events, this can have a noticeable effect on inference in power-law testing, and hence whether the goodness-of-fit is sufficiently high to be a power law or not. For example, Zwetsloot (2018) tests for power laws using the ACLED (Armed Conflict Location & Event Data Project) which is even less appropriate for this purpose than is the GED database if one does not first remove the composite events. ACLED has the practice of simply coding 10 deaths whenever the real number of people killed in an event is unknown, thereby creating a database that mixes together true events with many other that are, essentially, fabricated 10's.

2 Beyond Power Laws: Generative Theory

As suggested earlier, many conflict event datasets are well fit by power-laws with exponent values clustering around 2.5 (Bohorquez et al., 2009; Johnson et al., 2013; Spagat et al., 2018), and with p-values well above standard rejection thresholds for a power-law test. However Bohorquez et al. (2009) noted that there are important deviations from this approximate power-law pattern and explicitly present a two-population model featuring conflict between Red and Blue populations (see inset Fig. 5). As well as capturing the approximate power-law shape and slope in the event size distributions, Fig. 5 illustrates how this multi-sided generative model also reproduces the conflict-dependent deviations *beyond* a power law. The solid curves in Fig. 5 show this explicitly. Bohorquez et al. (2009) and Johnson et al. (2013) go on to discuss how a more basic one-population version of this model can be solved mathematically using calculus, to reproduce the approximate 2.5 empirical exponent value. This is shown in the Appendix, and is obtained by replacing the impact of the Blue population by a probability of Red cluster fragmentation. The full model — i.e. the two-population version of the model — goes much further by also explaining the deviations at low and higher casualty numbers, and hence the deviations from a power-law as shown in Fig. 5. A closer examination of the agent-based dynamics in the model shows that the ratio between the two populations' strengths (Red and Blue) tends

to control the general behavior of the slope, with greater strength differences resulting in steeper slopes, while the total Red strength tends to control the large high-end roll-off in Fig. 5 (Bohorquez et al., 2009).

3 Conclusion

We have reviewed how computational data science techniques and agent-based modeling can now shed new light on the age-old issue of human conflict. We also provided three contributions which help unify disparate existing claims in the literature, and support the notion of a unified framework for understanding human conflict. We showed that the approximate power law obtained for whole war sizes bears a simple relationship to the approximate power laws obtained from events within individual wars. Our finding that looking at individual violent events within a single war is therefore not the same as looking at individual wars within a collection of many wars, serves as a warning to computational science in general – that numerical statistical signatures can depend on the way in which data is collected and binned. More importantly, our finding overturns apparent assumptions in the literature (see for example Clauset (2018)) that the behavior over aggregated conflicts is somehow separate from the behavior within wars, due to their different power-law exponents. We note in passing that we have also tried hard to reproduce this effect analytically, whereby aggregating over all conflicts produces another approximate power law distribution but now with a different power-law exponent. We have not yet been able to do so, and hence we leave this as a challenge to the scientific community as an interesting and open mathematical problem. We also clarified some misunderstandings relating to the application of power-law estimation and testing procedures to the messy conflict datasets available to modern researchers.

We also reviewed how a generative theory of human conflict can be provided that reproduces the observed casualty distributions but does not make any implicit assumptions about power-law behavior. Not only can it replicate the approximate power-law behaviors, it also provides a quantitative explanation of deviations from pure power laws of these distributions and relates it to the dynamics of the conflict.

We believe that this data driven and computational science approach could

help intervene in human conflict in two ways. The first way is to use the approximate power-law universality over all conflicts (i.e. power-law exponent $\alpha \sim 1.5 - 1.7$) and the power law within single conflicts (i.e. power-law exponent $\beta_i \sim 2.5$) to make order-of-magnitude predictions concerning what to expect in terms of casualties across and within future conflicts respectively. For example, the approximate power-law functional form of the single conflict distribution (i.e. $Cs^{-\beta_i}$ for $s > s^i_{\min}$) can be used to calculate analytically an estimate for the expected number of casualties in the next event within an ongoing conflict or terrorist campaign, given by $[(\beta_i - 1)/(\beta_i - 2)]s^i_{\min}$ where $s^i_{\min}$ is the event size above which the power-law applies. Choosing $\beta_i = 2.5$ and $s^i_{\min} = 50$ as illustration, yields the expected number of casualties in the next event to be 150. This can help with planning in terms of dealing with casualties, and may conceivably even act as a partial deterrent for initiating such a future event. A consequence of our accompanying dynamical cluster theory (see Appendix) is that a state army can avoid having to find and destroy the largest (i.e. most lethal) insurgent clusters, by instead regularly breaking up smaller (i.e. less powerful) ones. The second way focuses on relating the deviations from perfect universality to the narrative of a specific conflict, i.e. it provides benchmark results against which specific conflicts (Fig. 2) or terrorist organization activity (Fig. 3) can be compared to see how and why they may deviate. For example, if a specific conflict deviates from the benchmark 2.5 approximate power-law either by having a very low p value and/or a β value far from 2.5, then a specific narrative of this conflict could be used to explain why the mechanism in that conflict might be different from the others, and hence different from the generative mechanism presented in the Appendix. We see this as a particularly attractive way to bring together the computational science and social science communities around the topic of human conflict and terrorism studies.

Appendix

We now review, for completeness, the basic one-population version of our generative model in the inset in Fig. 5 and discussed in Sec. 2. It focuses on the Red population and their clustering dynamics. To simplify the multi-sided nature of the generative model, we replace the feature that clusters fragment when interacting with Blue, or when sensing imminent danger, by simply

assigning a probability for the Red clusters to fragment. As we show below, this yields an exponentially cutoff 2.5-exponent power-law for the distribution of Red cluster sizes. If we then assume that the civilian population represents a passive background that simply absorbs the strength of each Red cluster when that Red cluster acts, the distribution of civilian casualties should have a similar distribution to that of the insurgent (i.e. Red) clusters. The internal coherence of a population of N objects (which we refer to as an 'agents' to acknowledge potential future application to human and/or cyber systems) comprises a heterogenous soup of clusters, at each timestep. Within each cluster, the component objects have a strong intra-cluster coherence. The inter-cluster coherence is weak between clusters. An agent i is then picked at random, or equivalently a cluster is randomly selected with probability proportional to size. Here we let s_i be the size of the cluster to which this agent belongs. The probability $\nu_{\rm frag}$ is the probability that the coherence of a given cluster fragments completely into s_i clusters of size one. If it doesn't fragment, then a second cluster is randomly selected with probability again proportional to size, or equivalently another agent j is picked at random. With probability $\nu_{\rm coal}$, the two clusters then coalesce – or equivalently this can be thought of them developing a common 'coherence' in their thinking or activities.

We start with the Master Equation for these cluster dynamics:

$$\frac{\partial n_s}{\partial t} = \frac{\nu_{\rm coal}}{N^2}\sum_{k=1}^{s-1} k n_k (s-k) n_{s-k} - \frac{\nu_{\rm frag} s n_s}{N} - \frac{2\nu_{\rm coal} s n_s}{N^2}\sum_{k=1}^{\infty} k n_k \ , \quad s \geq 2 \quad (1)$$

$$\frac{\partial n_1}{\partial t} = \frac{\nu_{\rm frag}}{N}\sum_{k=2}^{\infty} k^2 n_k - \frac{2\nu_{\rm coal} n_1}{N^2}\sum_{k=1}^{\infty} k n_k \ . \quad (2)$$

We make an approximation that $N \to \infty$. The terms on the right hand side of Eq. (1) represent all the ways in which the number of clusters of size s, given by n_s, can change. Taking the steady state, we obtain:

$$s n_s = \frac{\nu_{\rm coal}}{(\nu_{\rm frag} + 2\nu_{\rm coal})N}\sum_{k=1}^{s-1} k n_k (s-k) n_{s-k} \ , \quad s \geq 2 \ , \quad (3)$$

$$n_1 = \frac{\nu_{\rm frag}}{2\nu_{\rm coal}}\sum_{k=2}^{\infty} k^2 n_k \ . \quad (4)$$

Consider

$$G[y] = \sum_{k=0}^{\infty} k n_k y^k = n_1 y + \sum_{k=2}^{\infty} k n_k y^k \equiv n_1 y + g[y] \ , \quad (5)$$

where y is a parameter and g[y] governs the cluster size distribution n_k for $k \geq 2$. Multiplying Eq. (3) by y^s and then summing over s from 2 to ∞, yields:

$$g[y] = \frac{\nu_{\rm coal}}{(\nu_{\rm frag} + 2\nu_{\rm coal})N} G[y] \ , \tag{6}$$

i.e.

$$g[y]^2 - \left(\frac{\nu_{\rm frag} - 2\nu_{\rm coal}}{\nu_{\rm coal}} N - 2n_1 y \right) g[y] + n_1^2 y^2 = 0 \ . \tag{7}$$

From Eq. (5), $g[1] = G[1] - n_1$. Substituting this into Eq. (7) and setting $y = 1$, we can solve for $g[1]$

$$g[1] = \frac{\nu_{\rm coal}}{\nu_{\rm frag} + 2\nu_{\rm coal}} N \ . \tag{8}$$

Hence

$$n_1 = N - g[1] = \frac{\nu_{\rm frag} + \nu_{\rm coal}}{\nu_{\rm frag} + 2\nu_{\rm coal}} N \ . \tag{9}$$

Substituting this into Eq. (7) yields

$$g[y]^2 - \left(\frac{\nu_{\rm frag} + 2\nu_{\rm coal}}{\nu_{\rm coal}} N - \frac{2N(\nu_{\rm frag} + \nu_{\rm coal})}{\nu_{\rm frag} + 2\nu_{\rm coal}} y \right) g[y] + \frac{(N(\nu_{\rm frag} + \nu_{\rm coal}))^2}{(\nu_{\rm frag} + 2\nu_{\rm coal})^2} y^2 = 0 \, . \tag{10}$$

This quadratic can now be solved for $g[y]$

$$g[y] = \frac{(\nu_{\rm frag} + 2\nu_{\rm coal})N}{4\nu_{\rm coal}} \left(2 - \frac{4(\nu_{\rm frag} + \nu_{\rm coal})\nu_{\rm coal}}{(\nu_{\rm frag} + 2\nu_{\rm coal})^2} y - 2\sqrt{1 - \frac{4(\nu_{\rm frag} + \nu_{\rm coal})\nu_{\rm coal}}{(\nu_{\rm frag} + 2\nu_{\rm frag})^2} y} \right) \ , \tag{11}$$

which can then be written out as

$$g[y] = \frac{(\nu_{\rm frag} + 2\nu_{\rm coal})N}{2\nu_{\rm coal}} \sum_{k=2}^{\infty} \frac{(2k-3)!!}{(2k)!!} \left(\frac{4(\nu_{\rm frag} + \nu_{\rm coal})\nu_{\rm coal}}{(\nu_{\rm frag} + 2\nu_{\rm coal})^2} y \right)^k \ . \tag{12}$$

We now compare with the definition of $g[y]$ in Eq. (5), leading to

$$n_s = \frac{\nu_{\rm frag} + 2\nu_{\rm coal}}{2\nu_{\rm coal}} \frac{(2s-3)!!}{s(2s)!!} \left(\frac{4(\nu_{\rm frag} + \nu_{\rm coal})\nu_{\rm coal}}{(\nu_{\rm frag} + 2\nu_{\rm coal})^2} \right)^s \ . \tag{13}$$

Then making use of Stirling's series, we obtain

$$ln[s!] = \frac{1}{2} ln[2\pi] + \left(s + \frac{1}{2} \right) ln[s] - s + \frac{1}{12s} - ... \ . \tag{14}$$

Hence for $s \geq 2$, we find

$$n_s \approx \left(\frac{(\nu_{\text{frag}} + 2\nu_{\text{coal}})e^2}{2^{3/2}\sqrt{2\pi}\nu_{\text{coal}}} \right) \left(\frac{4(\nu_{\text{frag}} + \nu_{\text{coal}})\nu_{\text{coal}}}{(\nu_{\text{frag}} + 2\nu_{\text{coal}})^2} \right)^s \frac{(s-1)^{2s-3/2}}{s^{2s+1}} N \ , \qquad (15)$$

which gives

$$n_s \sim \left(\frac{\nu_{\text{coal}}^{s-1}(\nu_{\text{frag}} + \nu_{\text{coal}})^s}{(\nu_{\text{frag}} + 2\nu_{\text{coal}})^{2s-1}} \right) s^{-5/2} \quad . \qquad (16)$$

For $s \gg 1$, which means larger cluster sizes such as in the tail of the distribution, this is the same as saying

$$n_s \sim \exp(-s/s_0) s^{-5/2} \qquad (17)$$

where

$$s_0 = -\left[\ln \left(\frac{4(\nu_{\text{frag}} + \nu_{\text{coal}})\nu_{\text{coal}}}{(\nu_{\text{frag}} + 2\nu_{\text{coal}})^2} \right) \right]^{-1} \quad . \qquad (18)$$

The power law behavior is dominated by the exponential function for large cluster sizes (i.e. large s such that $s \sim O(N)$). Then the equilibrium state for the distribution of cluster sizes can therefore be considered a power-law with exponent $\alpha \sim 5/2 = 2.5$ together with an exponential cut-off. This model captures the fact that the interactions in future conflicts, given the advances in communications technology, will likely be effectively distance-independent, i.e. it captures the fact that messages can be transmitted over arbitrary distances. There are many generalizations that can be added to the model and yet give the same result, which confirms the robustness of this 2.5 result. An even wider variety of exponents very similar to the range of empirical findings in Figs. 1-3, emerges if we then allow a generalized form for the rigidity of clusters (i.e. probability of a picked cluster coalescing or fragmenting) such that it depends on size. In this case, the exponent is expected to vary typically from 1.5 to about 3.5, which is consistent with the observed range in Figs. 2-3.

We are very grateful to past students and post-docs who were part of this research program and contributed to the understanding and results shown here.

References

Bohorquez, J. C., S. Gourley, A. R. Dixon, M. Spagat, and N. F. Johnson (2009). Common ecology quantifies human insurgency. *Nature 462*(7275), 911.

Braumoeller, B. F. (2019). *Only the Dead: The Persistence of War in the Modern Age*. Oxford University Press, USA.

Cederman, L.-E. (2003). Modeling the size of wars: From billiard balls to sandpiles. *American Political Science Review 97*(1), 135–150.

Clauset, A. (2018). Trends and fluctuations in the severity of interstate wars. *Science Advances 4*(2), eaao3580.

Clauset, A., M. Young, and K. S. Gleditsch (2007). On the frequency of severe terrorist events. *Journal of Conflict Resolution 51*(1), 58–87.

Gillespie, C. S. (2015). Fitting heavy tailed distributions: The poweRlaw package. *Journal of Statistical Software 64*(2).

González-Val, R. (2016). War size distribution: Empirical regularities behind conflicts. *Defence and Peace Economics 27*(6), 838–853.

Johnson, N. F., P. Medina, G. Zhao, D. S. Messinger, J. Horgan, P. Gill, J. C. Bohorquez, W. Mattson, D. Gangi, H. Qi, et al. (2013). Simple mathematical law benchmarks human confrontations. *Scientific Reports 3*, 3463.

Richardson, L. F. (1948). Variation of the frequency of fatal quarrels with magnitude. *Journal of the American Statistical Association 43*(244), 523–546.

Richardson, L. F. (1960). *Statistics of deadly quarrels*, Volume 1960. Boxwood Pr.

Spagat, M., N. F. Johnson, and S. van Weezel (2018). Fundamental patterns and predictions of event size distributions in modern wars and terrorist campaigns. *PLoS One 13*(10), e0204639.

Zwetsloot, R. (2018). Testing Richardson's Law: A (cautionary) note on power laws in violence data. *Available at SSRN 3112804*.

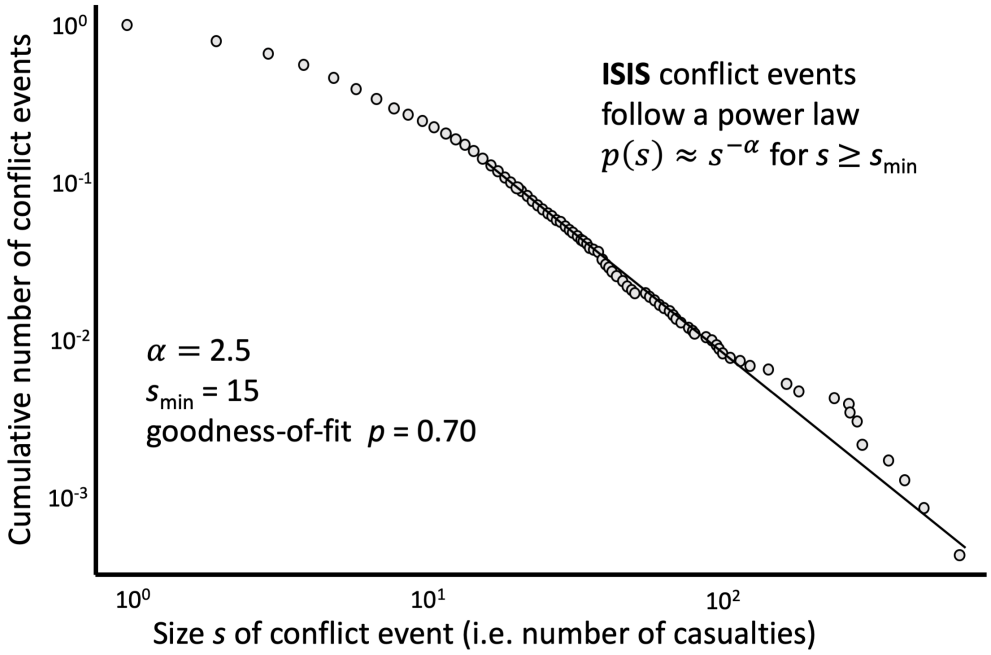

Figure 1: Histogram for attacks involving ISIS, follows a power law to a good approximation. The number of events of a given size or larger are shown on the y axis. Event sizes are given by the number of casualties, which are plotted on the x-axis. The plot shows the cumulative total, and the solid line indicates the best-fit power law.

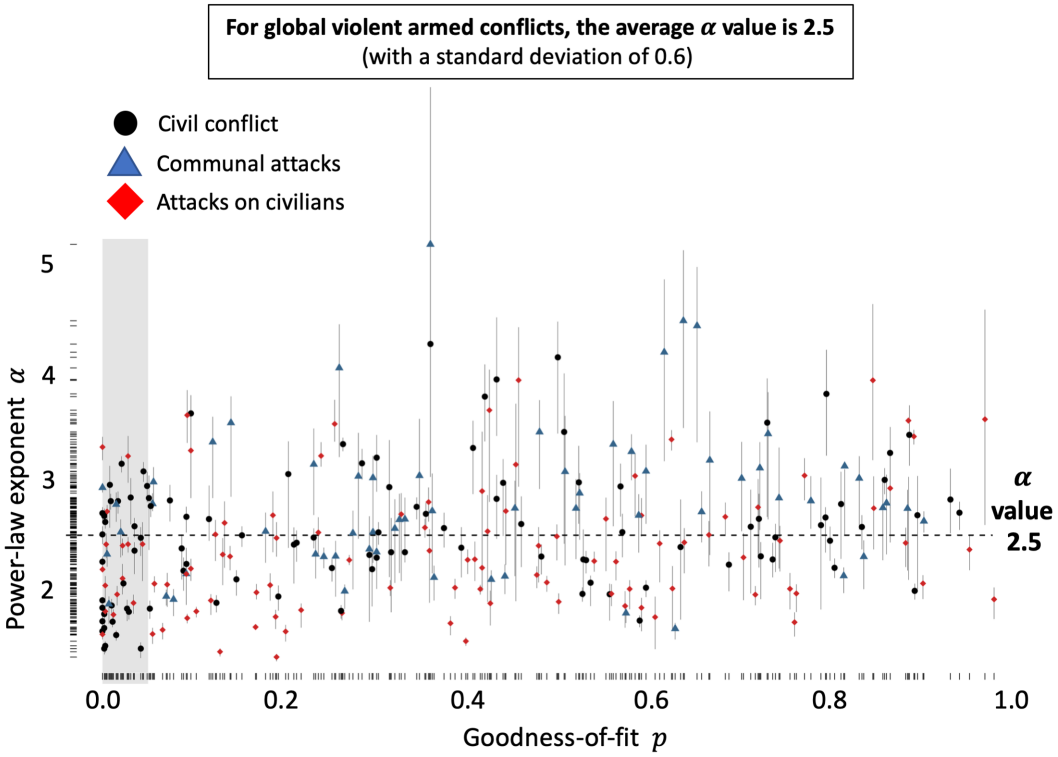

Figure 2: Plot shows (vertical axis) estimates of α parameter, along with 50 percent uncertainty interval, versus (horizontal axis) goodness-of-fit p values for power-law hypotheses for global violent armed conflicts. Grey shaded area corresponds to goodness-of-fit $p \leq 0.05$. Adapted from the authors own original figure as appearing in Spagat et al. (2018), which permits unrestricted use under the terms of the Creative Commons Attribution License.

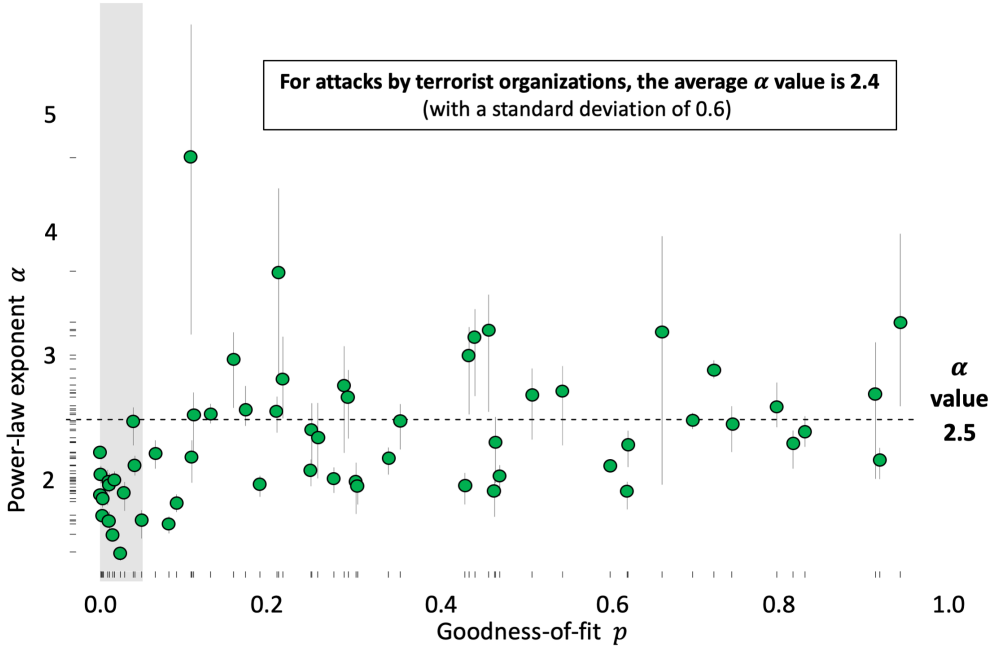

Figure 3: Plot shows (vertical axis) estimates of α parameter, along with 50 percent uncertainty interval, versus (horizontal axis) goodness-of-fit p values for power-law hypotheses for terrorist organizations. Grey shaded area corresponds to goodness-of-fit $p \leq 0.05$. Adapted from the authors own original figure as appearing in Spagat et al. (2018), which permits unrestricted use under the terms of the Creative Commons Attribution License.

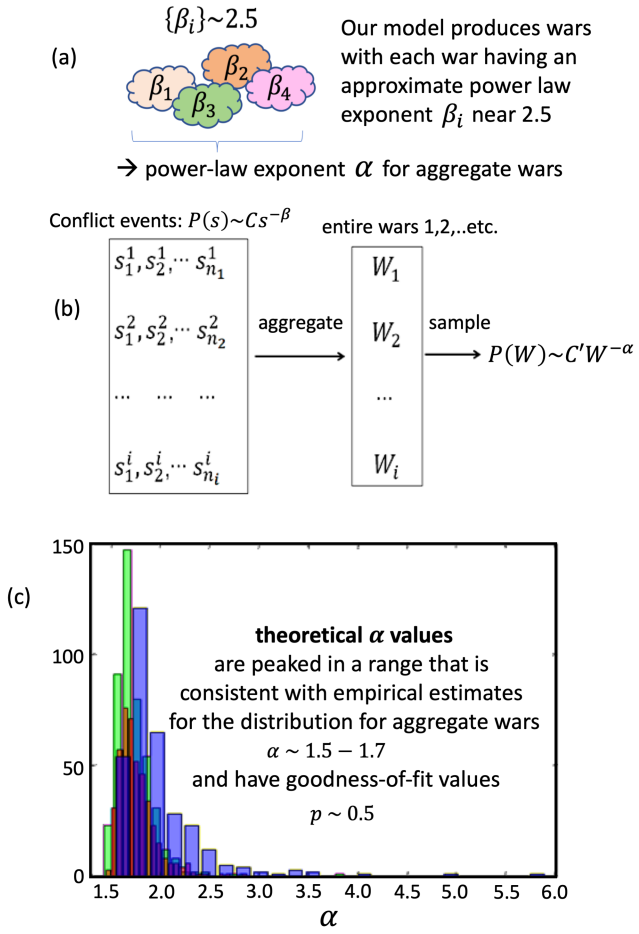

Figure 4: (a) Schematic of the simulation procedure, shown in more detail in (b). To generate a number of wars consistent with our model, we generate events from power-law distributions with exponents distributed around 2.5 (see text). The aggregate size of each war is calculated, yielding $\{W_i\}$. This set of $\{W_i\}$ values is then sampled to mimic the process of using a database of known wars with known aggregate totals. As shown in (c), the resulting power law exponents for the aggregate size of entire wars, is in the range observed empirically. Each distribution is for a different number of mean events per war. In each case, the distribution of α values tends to be peaked in a range that is consistent with the empirical values for entire wars (i.e. $\alpha \sim 1.5 - 1.7$) and they each have reasonably high goodness-of-fit values p ($p \sim 0.5$).

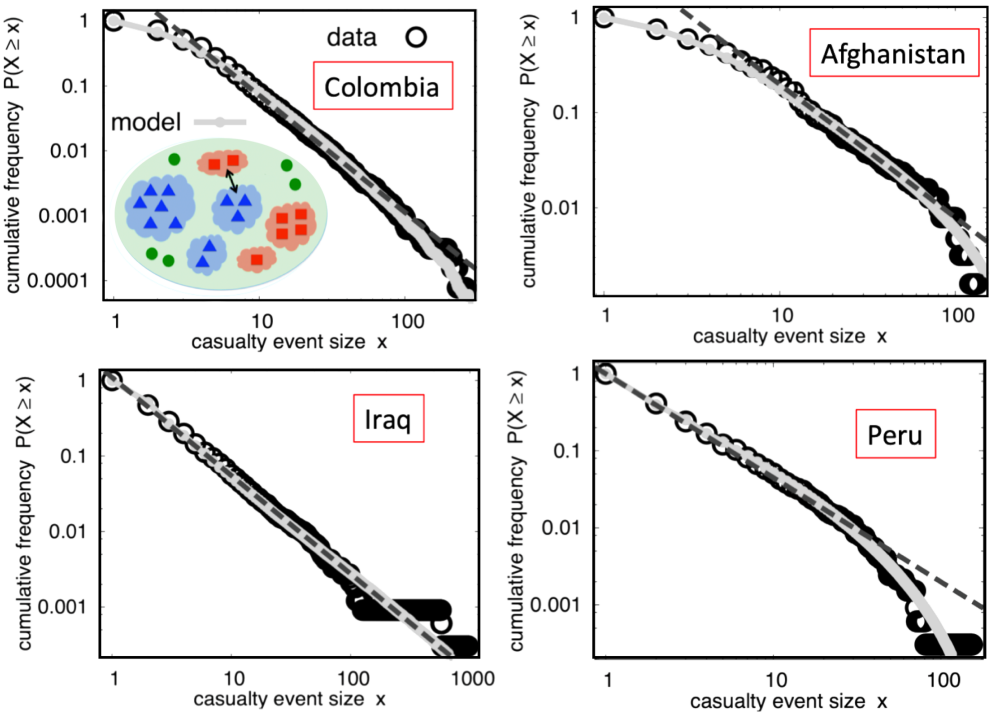

Figure 5: The behavior across four example conflicts, of the complementary cumulative distribution of event size $P(X \geq x)$ where x is the number of casualties in an event within the conflict. We have adapted this figure from Bohorquez et al. (2009). The results from our generative model (shown as an inset and discussed in Sec. 2) are shown as solid, light gray curves. The inset shows schematically our generative model which is a two-population Red-Blue conflict: clusters of red squares and clusters of blue triangles that interact, together with Greens (green circles) who are passive civilians. The dashed line is a straight line guide-to-the-eye: it is not a power-law fit.